Non-linear grey-box modelling for heat dynamics of buildings

Thilker, Christian Ankerstjerne; Bacher, Peder; Bergsteinsson, Hjörleifur G.; Junker, Rune Grønborg; Cali, Davide; Madsen, Henrik

Published in:
Energy and Buildings

Link to article, DOI:
10.1016/j.enbuild.2021.111457

Publication date:
2021

Document Version
Publisher's PDF, also known as Version of record

Energy & Buildings 252 (2021) 111457

Contents lists available at ScienceDirect

Energy & Buildings

journal homepage: www.elsevier.com/locate/enb

Non-linear grey-box modelling for heat dynamics of buildings

Christian Ankerstjerne Thilker *, Peder Bacher, Hjörleifur G. Bergsteinsson, Rune Grønborg Junker, Davide Cali, Henrik Madsen

Technical University of Denmark, Department of Applied Mathematics and Computer Science, Asmussens Allé, Building 303B, DK-2800 Kgs. Lyngby, Denmark

ARTICLE INFO

Article history:
Received 28 June 2021
Revised 28 August 2021
Accepted 9 September 2021
Available online 16 September 2021

Keywords:
Grey-box models
Stochastic differential equations
Non-linear models
District heating
Smart energy systems

ABSTRACT

This paper introduces a non-linear grey-box (GB) model based on stochastic differential equations that describes the heat dynamics of a school building in Denmark, equipped with a water-based heating system. The building is connected to a local district heating network through a heat exchanger. The heat is delivered to the rooms mainly through radiators and partially through a ventilation system. A monitoring system based on IoT sensors provides data on indoor climate in the rooms and on the heat load of the building. Using this data, we estimate unknown states and parameters of a model of the building's heating system using the maximum likelihood method. Important novelties of this paper include models of the water flow in the circuit and the state of the valves in the radiator thermostats. The non-linear model accurately predicts the indoor air temperature, return water temperature and heat load. The ideas behind the model lay a foundation for GB models of buildings that use different kinds of water-based heating systems such as air-to-water/water-to-water heat pumps. Such GB models enable model predictive control to control e.g. the indoor air climate or provide flexibility services.

1. Introduction

The use of fossil-based energy sources does not belong in a sustainable future [1]. Society must shift to energy sources where CO_2-emissions lie within the planetary boundaries; i.e. we need to use resources that are renewable [2]. This future low-carbon society calls for fundamental changes of the energy system. Today the systems are operated such that the production follows the demand. However, an efficient implementation of a low-carbon society calls for a system where the demand follows the weather-driven energy production. Most importantly we need methods for unlocking the flexibility at all levels of the society; examples being buildings, supermarkets, wastewater treatment plants, industrial process facilities, districts, municipalities and cities. A lot of recent work, therefore, centres around the concept known as energy flexibility [3,4]. The core idea is to control the energy consumption to align it with energy production. For this purpose, model-based predictive control is a very promising control framework [5]. This paper introduces a novel grey-box (GB) model based on stochastic differential equations (SDEs) that is designed for controller based optimisation of the heat load of buildings. The ultimate purpose of developing such a GB model is to intelligently control buildings in order to minimise the CO_2-emissions and unlock the flexibility. A reliable model (together with weather forecasts) is essential for a good performance of model predictive control (MPC) for buildings [6].

Complex building energy performance models based exclusively on physical equations, known as white–box models, are often used for providing simulations. Occasionally, in white box building models, stochastic models are used to simulate occupants behaviour, as in [7,8]. However, they are demanding to build, computationally heavy, and difficult or impossible to tune to real-world data, which makes them infeasible for control. Especially for the existing building stock. On the contrary, black–box models can be fast in terms of simulation time. But they do not include laws of physics, and thus may be hard to interpret and lack the ability to extrapolate and generalise beyond training data. GB models bridge the gap between white- and black-box models by leveraging both physical and statistical properties [9]. They are based on *simple* physical principles and considerations of the system, which make them computationally light and ideal for parameter calibration using available data. Linear GB models for buildings are widely seen in the literature [10]. Wang and Xu [11] use a genetic algorithm to estimate a linear heat dynamics model that describes the thermal conditions in the wall envelopes and internal mass for an office building. The goal is to predict the heat load and the indoor air temperature. Massano et al. [12] uses an unscented Kal-

* Corresponding author.
E-mail addresses: chant@dtu.dk (C.A. Thilker), pbac@dtu.dk (P. Bacher), hgbe@dtu.dk (H.G. Bergsteinsson), rung@dtu.dk (R.G. Junker), dcal@dtu.dk (D. Cali), hmad@dtu.dk (H. Madsen).

https://doi.org/10.1016/j.enbuild.2021.111457
0378-7788/

Nomenclature

$T_t^{(i,j)}$	Indoor air temperature in room i
T_t^i	Mean indoor air temperature
T_t^{for}	Forward/supply water temperature
T_t^{ret}	Return water temperature
T_t^{set}	Set-point of the radiator thermostats
ϕ_t^h	Heat load of the building
T_t^a	Outdoor air temperature
ϕ_t^s	Global solar radiation on a horizontal surface
T_t^w	Temperature of building wall to the outside
T_t^h	Temperature of the radiators
A_w	The effective window area of the building
ω_t	Brownian motion
T_{offset}	A temperature offset between the thermostats and the observation sensors
f_t^{valve}	The valve opening state (on a scale of 0 to 1)
Φ_t	The flow of the water in the radiator circuit
$\Phi_{\max}$	The maximum flow of the water in the radiator circuit
$c_{p,w}$	The specific heat capacity of water
$\mathbf{X}_k$	The stochastic state variable of the building system at time t_k
$\mathbf{Y}_k$	The stochastic observation variable of the building system at time t_k
C_i	Heat capacity of the indoor air
C_w	Heat capacity of the building wall
C_f	A "weight" on the water flow, which determines how fast the water accelerates
C_h	Heat capacity of the radiators
R_{ih}	Heat transfer resistance between the indoor air and the radiators
R_{iw}	Heat transfer resistance between the indoor air and the building walls
R_{wa}	Heat transfer resistance between the indoor air and the outdoor air
R_{fr}	Heat transfer resistance between the radiators and the return temperature

man filter to estimate parameters in a linear RC-inspired model to predict the indoor air temperature. Bacher and Madsen [13] outlines a model development procedure for stochastic differential equation (SDE)-based GB models. However, it is a well known fact that *non-linear systems* exhibit vast richness in the solution structure, far beyond what is seen in linear systems [14]. For instance, non-linear models are necessary to sufficiently describe the heat dynamics of building integrated photo-voltaic modules [15,16]. Non-linear GB models can also be found within industrial robotics [17] and in aquatic ecosystems modelling [18], just to mention a few areas. To the knowledge of the authors, the literature on non-linear GB models for radiator-based heating systems is scarce.

We propose SDEs as the modelling framework for the building model [19]. This has many advantages: First, SDEs provide a natural method to model physical phenomena as they are formulated in continuous-time. Second, they include probabilistic uncertainty that accounts for modelling approximations, unrecognised exogenous variables, and uncertainty related to the provided input variables. Last, they lay a solid foundation providing predictions of the system behaviour and for model-based optimal control, to predict system behaviour. It is well-know that solutions to Ordinary Differential Equations (ODEs) are functions of time, and this implies that an ODE modelling framework assumes that we are able to predict the exact evolution in time of the states. Solutions to SDEs are stochastic processes, which are characterised by the family of finite-dimensional densities, and this implies that the future evolution of the states is encumbered with uncertainty, and this uncertainty can be quantified. Optimal control theory based on SDEs is well-established in the literature with numerous examples of applications, e.g. for control of glucose concentration in humans [20], building thermal control [21], and operation of waste-water treatment plants [22].

1.1. Main contributions

The existing literature contains various examples of linear GB models of the heat dynamics of buildings. However, the literature seems to contain limited work on SDE-based non-linear GB models for water-based heating systems, especially related to district heating (DH). This paper presents and analyses the development of a non-linear GB model for a school building in Denmark with water-based heating. We base the analysis and estimation on a single week of data using meteorological weather observations as inputs, and we will demonstrate that one week of data is sufficient for identifying a good model. Due to the generality of the model, it is argued that the model is applicable to a wide range of buildings with water-based heating systems and different heat sources (including heat pumps).

An important contribution of this paper is the model of the thermostatic valves of the radiators. The radiator valves are mechanically adjusted by the thermostats that are configured with a set-point. The valves open and close proportionally to the difference between the set-point and actual air temperature. The valves naturally do not behave discontinuously when heat is or is not needed. Models for thermostatic valves exist in applications of white-box models [23]. Most are modelled as P, PI, or PID-based controllers for white-box building models [24]. Hansen [25] suggested detailed physical models of radiators and thermostats. However, the models end up being too large and detailed for grey-box purposes. To the knowledge of the authors, the literature contains no examples of models for thermostat valves formulated as GB-models. This paper presents a sigmoid-function to describe the continuous sensitivity of the valves due to changes in the indoor air temperature according to the set-point. Another important contribution is a model of the water flow in the building heating system.

1.2. Structure and outline of the paper

This paper has the following structure. Section 2 introduces the building and its engineering systems, together with the overall experiment. Here, we also describe the data and how it was gathered. Section 3 describes the model development process and the ideas behind the suggested model. Next, we present and discuss the results; the parameter estimates, a simulation of the variables compared to data, and a 1-step residual analysis. Lastly, Section 6 sums up the essential findings of the paper.

2. The building and the experimental setup

This section introduces the building and describes the experimental data and the generation process.

2.1. The building

The building, a school with three floors and a basement, is located in Høje Taastrup, Denmark. The uppermost floor is a part-refurbished roof attic. Bruun [26] provides all technical information about the building.

Being built in 1929, the building is not insulated according to modern standards. Fig. 1 shows a digital reconstruction and a photo of the building. It includes 10 classrooms that are ventilated by mechanical ventilation using an air handling unit (AHU) for air circulation. The facade and internal walls consist of solid bricks (300 mm and 180 mm thickness, respectively). The windows have wooden frames and double-paned low-E glazings. Floors are made from wood joists and the roof is partly uninsulated and partly insulated slate roof. The building is connected to the local electricity and heat grid, where the ladder is a DH system. The building uses district heating for domestic hot water (DHW), the AHU, and space heating. The latter term governs the heating (and cooling) system of the indoor air. For this building, the space heating is a separate water-based circuit with dedicated pumps. Radiators of different types (cast-iron, panel convectors, plane conductors) with individual thermostats establish the space heating system in the individual rooms of the building. Individual thermostatic valves automatically regulate the water flow into the radiator units as to maintain a pre-defined *set-point*. The space heating system is separated from the DH system by a plate heat exchanger. Independent PI-controllers regulate the water flow on both the district heating and the building side of the heat exchanger.

2.2. The experiment

The experiment carried out was planned in advance and designed to generate data suitable for system identification purposes. The main focus was to change the control input, the thermostat set point, such that information about the essential dynamics of the system can be estimated. A sequence of the set point was designed with four different parts. First part contains a few long steps with set points set to a minimum (10 °C) and back again to a base level (21 °C) to get information about the dynamics governing the system. Second part is a multilevel signal, where the extremes (14 and 27 °C) are kept for the longest time and then shorter periods are kept for relatively shorter time. Third part contains short periods with drops to a minimum from the base temperature. Finally, a step sequence where the set point is stepped from 23 °C in two hours steps down to 17 °C and up again. The forward temperature of the space heating water is set constant to 55 °C at all times. The entire sequence was slightly shorter than 7 days and was executed during the Christmas vacation, where the building was unoccupied.

Fig. 1. Visual illustrations of the building site. The upper digital reconstruction is supplied by [26].

2.3. The data

Table 1 lists all the variables of the data. Fig. 2 shows the experimental data in the period December 21 through December 27. The upper graph displays the heat load of the building. It seems to be characterised by a large peak whenever the heat turns on, before reverting to a lower and steady level. The second graph shows the forward- and return water temperature, which go to and from the space heating system. The forward temperature was set constant to 55 °C during the entire experiment. The forward temperature fluctuates a lot, though, when the thermostat set point is set very low – because the thermostat valves are closed, the flow in the radiator circuit is nearly stopped, which results in inappropriate oscillations of the forward temperature since the PI controllers were not designed for this situation. But it plays no role, since the water flow is near zero during these times. The return temperature quickly becomes large when the space heating is turned on. In absence of heat load, the return temperature quickly decreases. But, the reversion and behaviour in absence of heat load seem to be rather inconsistent. The third graph shows the indoor temperature of each room (in blue) and the mean of all rooms (in black). Lastly, the bottom graph shows the exterior weather conditions, i.e. the outdoor air temperature and the global solar radiation. The latter is relatively small throughout the period, which complicates the estimation of the solar radiation gain for the model. We return to this matter later in Section 5.

The variables of the building we wish to be able to predict are the following.

- The mean indoor air temperature, T_t^i.
- The heat load of the building delivered by the DH system, ϕ_t^h.
- The temperature of the returning water in the SH system of the building, T_t^{ret}.

The subscript t indicates the dependence on time. These variables are of special interest when it comes to optimal control of the indoor climate. In Denmark, building operators pay for the amount of heat they consume. Additionally, the operators pay fees for too high return temperatures since it is a source of poor energy efficiency in the DH network. First, the DH operators have to

Table 1
Data interpretation.

Name	Quantity	Unit
$T_t^{(i,j)}$	Indoor air temperature in room j	[°C]
T_t^i	Mean indoor air temperature in the building	[°C]
T_t^{for}	Forward temperature	[°C]
T_t^{ret}	Return temperature	[°C]
T_t^{set}	Temperature set-point	[°C]
ϕ_t^h	Delivered heat to the building	[kW]
T_t^a	outdoor air temperature	[°C]
ϕ_t^s	Solar radiation on a horizontal surface	[kW/m^2]

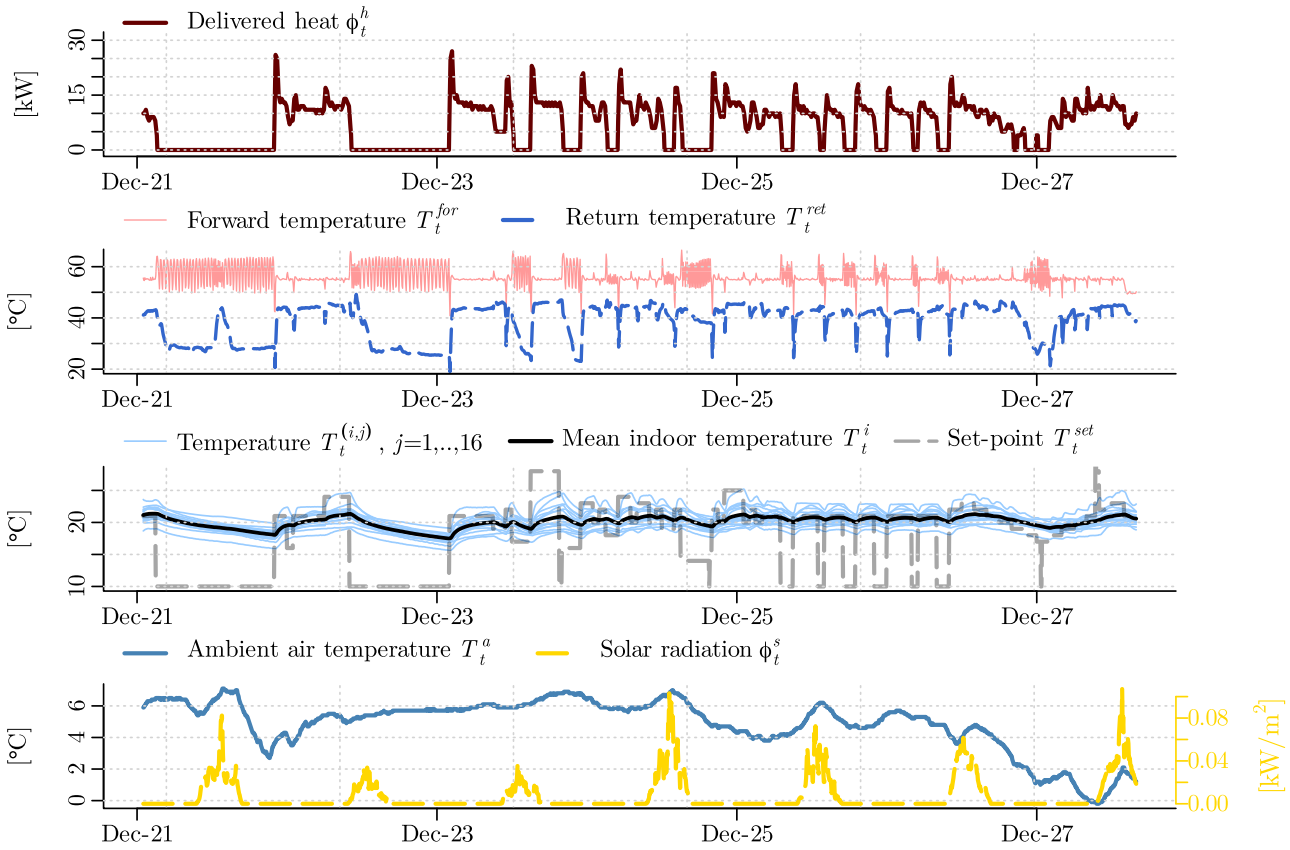

Fig. 2. The data from the experiment performed in December 2019.

increase the mass flow rate of the water, if the users do not cool the return water. Secondly, if the return water to the DH facilities is too hot, the efficiency of the central heat production plant decreases. This payment scheme makes it economically advantageous for the building operators to use heat when it is cheap and minimise the return temperature.

3. Model development

This section describes the model development process. Due to the complexity of the building and its systems, it is necessary to use a relatively big model. The dimensions of the state and parameter set of the model thus become rather high. To easier identify the necessary dynamics to include in the model and estimate initial values for the parameters, it is advantageous to split the modelling into several steps. The main idea is to split up the modelling processes into two parts. To identify the steps, we need to realise that the building heat dynamics consist of two parts (as a first simple assumption). The delivered heat from the water in the radiator system operates independently and only interacts with the indoor air temperature of the building by the radiators themselves. This interaction involves only two parameters. Therefore, we split the modelling part into the following three steps:

1. Given the observed time series of the delivered heat from the district heating system, we develop a model that predicts only the indoor air temperature of the building.
2. Given the observed time series of the indoor air temperature and set point, we develop a model that predicts only the heat load from the district heating system to the building. That is while keeping the parameters fixed, that concerns the indoor air temperature model obtained in step 1.
3. We combine the two models and start the parameter optimisation from the results of the two independently sufficient models to obtain a combined model structure.

By developing the two system models individually at first, it also becomes much easier to identify the necessary dynamical features that govern the systems.

3.1. Stochastic differential equations

The model will be formulated using SDEs. A SDE typically has the following form

$$\mathrm{d}\mathbf{X}_t = f(\mathbf{X}_t, t)\mathrm{d}t + g(\mathbf{X}_t, t)\mathrm{d}\boldsymbol{\omega}_t \tag{1}$$

where f and g are the drift and diffusion terms, respectively, and the subscript t denotes the dependence on time. The diffusion term makes a SDE differ from an ordinary differential equation. ω_t is known as Brownian motion and is a fundamental process for stochastic calculus. It is governed by independent Gaussian increments; $\omega_t - \omega_s \sim N(0, t-s)$, for $s \leqslant t$. This has remarkable consequences and relates it to the physical diffusion equation. The purpose of the diffusion term is to describe chaotic phenomena that are too complex to include in the drift part of the model structure.

3.2. The building heat dynamics model

The literature contains numerous examples of developing heat dynamic models for buildings using continuous-time GB models, see e.g. [27–31]. We do not give the model identification steps explicitly for our case though but simply report the final result.

Fig. 2 gives insights into what elements the building model should include. Inspections of the two long periods, where the heat

is turned off, show that the mean indoor temperature seems to drop fast at first and then flatten to a certain decay rate. This indicates that we should include two time constants; one for the fast and initial drop and one for the slow long-term decay. We may interpret these fast and slow dynamics as the temperature of the indoor air and the temperature of the building walls. For this reason, the wall exchanges heat with the ambient air and acts as a low-pass filter between the interior and exterior. We also choose to model the radiators as an accumulating medium where the heat input enters directly. We denote the indoor air temperature state T_t^i, the wall temperature state T_t^w, and the radiator temperature state T_t^h.The solar radiation gainϕ_t^s, enters into the room air directly through windows.

Fig. 3 shows the heat dynamics structure for the building as an RC-diagram. The equivalent SDE model has the following form

$$\mathrm{d}T_t^i = \frac{1}{C_i}\left(\frac{1}{R_{ih}}\left(T_t^h - T_t^i\right) + \frac{1}{R_{iw}}\left(T_t^w - T_t^i\right) + A_w\phi_t^s\right)\mathrm{d}t + \sigma_1\mathrm{d}\omega_t^1, \quad (2)$$

$$\mathrm{d}T_t^w = \frac{1}{C_w}\left(\frac{1}{R_{iw}}\left(T_t^i - T_t^w\right) + \frac{1}{R_{wa}}\left(T_t^a - T_t^w\right)\right)\mathrm{d}t + \sigma_2\mathrm{d}\omega_t^2, \quad (3)$$

$$\mathrm{d}T_t^h = \frac{1}{C_h}\left(\frac{1}{R_{ih}}\left(T_t^i - T_t^h\right) + \phi_t^h\right)\mathrm{d}t + \sigma_3\mathrm{d}\omega_t^3. \quad (4)$$

A_w is the effective window area (assumed constant), C_i, C_w, and C_h are heat capacities of the states, R_{ih}, R_{iw}, and R_{wa} are resistors between the heat media, and $\omega_t^k, k \in \{1,2,3\}$ are mutual independent Brownian motions.

3.3. The radiator circuit dynamics model

The thermostatic valves regulate the water flow through the radiators. An important novelty of this paper is to model the thermostatic valves using the non-linear sigmoid function. The idea is that the vales open when it is too cold and close when it is too warm. Assuming that the valves react continuously to the indoor air temperature, the sigmoid function corresponds to some kind of proportional control (0 being closed and 1 being open).

3.3.1. The thermostatic valve function

To describe the thermostatic control, i.e. the state of the valve in the radiator thermostats, we use a sigmoid function. To be specific, the thermostatic valve function describes the sensitivity of the heating system to deviations in the mean indoor air temperature. We use the following formulation

$$f_t^{\text{valve}} = \frac{1}{1 + \exp\left(-\alpha\left(T_t^{\text{set}} + T_{\text{offset}} - T_t^i\right)\right)}. \quad (5)$$

α is the slope of the sigmoid function and determines how quickly the heating system turns on and off. T_{offset} acts as an offset: since the observations of the indoor air temperature typically are not taken right next to the radiators, the thermostats may respond to a temperature that is warmer or colder than the observed one.

The sigmoid function has the disadvantage that it cannot reach 1 nor 0. For the purpose of this paper, it means that even though the set-point is, say, 18 and the observed temperature is 20, the model predicts that the radiators still deliver some heat (depending on the slope and offset). Depending on the specific thermostats and the valves in the radiators, this prediction may be wrong. We address this problem further in Section 5.

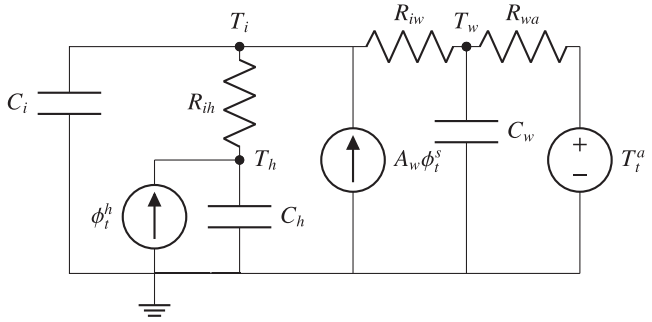

Fig. 3. The model structure of the building heat dynamics. The model predicts the indoor air temperature, $\hat{T}_i$, given the delivered power ϕ_h.

3.3.2. Derivation of the space heating model structure

The space heating system proved hard to model. It is difficult to describe all necessary dynamics in a simple manner. However, we found it fruitful to model the *water flow* in the radiator circuit as a dynamical equation governed by a time-delay. Since we do not observe the water flow in the radiators, we model it as a hidden state (which we need to estimate in the modelling). The governing physical equation of the net energy transferred to the radiator, Q_t^h, from the water is [24]

$$\mathrm{d}Q_t^h = \Phi_t c_{p,w}\left(T_t^{\text{for}} - T_t^{\text{ret}}\right)\mathrm{d}t \quad (6)$$

where Φ_t is the water flow in the SH system, $c_{p,w}$ is the specific heat capacity of water. We use (6) to model the heat delivered to the radiators (where the radiators in turn exchanges the heat with the indoor air). The above formulation does not consider that the flow rate in the individual radiators may be different due to e.g. different individual valve states or different positions in the building.

As Section 2.1 describes, pumps controlled by PI controllers regulate the water flow in the SH system to maintain a certain pressure. Therefore, there is a delay from when the valves open until the pumps increase the water accordingly. For this reason, it seems reasonable to model the water flow as a differential equation itself and let the flow be an individual state.

To model the return temperature, a few observations are important. It is obvious that when the space heating system delivers heat, the hot/cold water has been round in the radiator circuit and returns to the heat exchanger in a colder state. This is clearly visible in Fig. 2 that the return temperature varies between 40–50 °C when heat is delivered. However, when the heat load equals zero, the return temperature acts rather inconsistently. At these times, the return temperature mostly responds with a quick decay to below 30 °C. But as Fig. 2 shows, it sometimes drifts indescribably. Most times, when the water flow stops, the water in the return pipes quickly delivers its heat to the surroundings and arrives at some equilibrium. But when no heat is delivered, the building operators do not pay for larger return temperatures and gives no additional insights into the system. Therefore, we have no means to model the return temperature, when the heat load is zero. We thus disregard the return temperature observations when the flow is zero for simplicity. Section 5 explains how we implement this in the parameter estimation.

To recap the above thoughts; when heat is needed, the water flows into the radiators to deliver heat and afterward returns to the heat exchanger to be heated again. By combining (6) with a state for the flow and the return temperature, we arrive at the following model

$$\mathrm{d}\Phi_t = \frac{1}{C_f}\left(\Phi_{\max} f_{\text{valve}} - \Phi_t\right)\mathrm{d}t + \sigma_3\mathrm{d}\omega_t^3, \quad (7)$$

$$\mathrm{d}T_t^h = \frac{1}{C_h}\left(\Phi_t c_{p,w}\left(T_t^{\text{for}} - T_t^h\right) + \frac{1}{R_{ih}}\left(T_t^i - T_t^h\right)\right)\mathrm{d}t + \sigma_4\mathrm{d}\omega_t^4, \quad (8)$$

$$\mathrm{d}T_t^{\text{ret}} = \frac{1}{C_h}\left(\frac{1}{R_{fr}}\left(T_t^h - T_t^{\text{ret}}\right)\right)\mathrm{d}t + \sigma_5\mathrm{d}\omega_t^5. \quad (9)$$

where $\Phi_{\max}$ the maximum attainable flow of the radiator circuit water. Fig. 4 depicts the structure as a RC-diagram.

3.4. Heat load estimation equation

From (6) we estimate the heat load, i.e. the power from the DH to the indoor air, as

$$\phi_t^h = \Phi_t c_{p,w}\left(T_t^{\text{for}} - T_t^{\text{ret}}\right). \tag{10}$$

It should be natural to assume that the heat difference between the forward and return water is due only to the delivered heat by the space heating system. The temperature difference multiplied by the flow and the specific heat capacity of water is thus an estimate of the heat load. The flow state creates a time delay on the heat load. The term $\left(T_t^{\text{for}} - T_t^{\text{ret}}\right)$ is almost always large when the heat is turned off. Had there been no delay, e.g. for the equation $C_1 f_{\text{valve}}\left(T_t^{\text{for}} - T_t^{\text{ret}}\right)$, where C_1 is an arbitrary parameter, the heat load would immediately spike when the valves open. However, the heat load data is governed by delay which suggests that such time delay is needed.

3.5. The combined model

The combined model has the form

$$\mathrm{d}T_t^i = \frac{1}{C_i}\left(\frac{1}{R_{ih}}\left(T_t^h - T_t^i\right) + \frac{1}{R_{iw}}\left(T_t^w - T_t^i\right) + A_w\phi_t^s\right)\mathrm{d}t + \sigma_1\mathrm{d}\omega_t^1, \tag{11}$$

$$\mathrm{d}T_t^w = \frac{1}{C_w}\left(\frac{1}{R_{iw}}\left(T_t^i - T_t^w\right) + \frac{1}{R_{wa}}\left(T_t^a - T_t^w\right)\right)\mathrm{d}t + \sigma_2\mathrm{d}\omega_2, \tag{12}$$

$$\mathrm{d}\Phi_t = \frac{1}{C_f}\left(\Phi_{\max} f_{\text{valve}} - \Phi_t\right)\mathrm{d}t + \sigma_3\mathrm{d}\omega_t^3, \tag{13}$$

$$\mathrm{d}T_t^h = \frac{1}{C_h}\left(\Phi_t c_{p,w}\left(T_t^{\text{for}} - T_t^h\right) + \frac{1}{R_{ih}}\left(T_t^i - T_t^h\right)\right)\mathrm{d}t + \sigma_4\mathrm{d}\omega_t^4, \tag{14}$$

$$\mathrm{d}T_t^{\text{ret}} = \frac{1}{C_h}\left(\frac{1}{R_{fr}}\left(T_t^h - T_t^{\text{ret}}\right)\right)\mathrm{d}t + \sigma_t\mathrm{d}\omega_t^5. \tag{15}$$

where $\Phi_{\max}$ are the flow speed of the water on the building site. The observation equations are

$$y_k^i = T_{t_k}^i + v_1, \quad v_1 \sim N_{iid}(0, R_1), \tag{16}$$

$$y_k^h = \Phi_t c_{p,w}\left(T_t^{\text{for}} - T_t^{\text{ret}}\right) + v_2,\ v_2 \sim N_{iid}(0, R_2), \tag{17}$$

$$y_k^{\text{ret}} = T_{t_k}^{\text{ret}} + v_3,\ v_3 \sim N_{iid}(0, R_3). \tag{18}$$

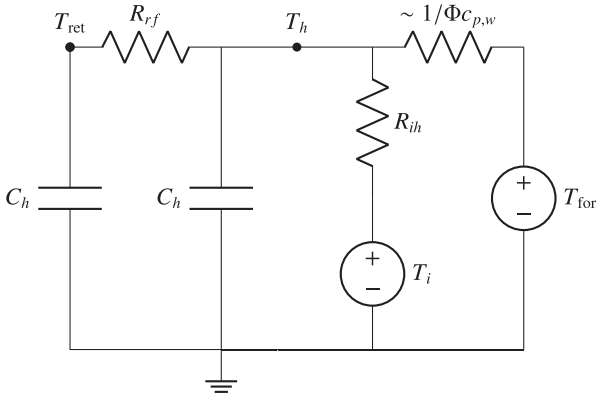

Fig. 4. The radiator circuit dynamics model visualised as an RC-diagram. The flow, Φ_t, acts as a heat transfer coefficient in the radiator temperature state. We simply write the resistance as the flow state Φ_t.

4. Model identification and estimation

This section describes the identification method and the details governing the parameter estimation process. This paper proposes maximum likelihood inference for parameter estimation in stochastic differential due to its ability to estimate noise parameters. See e.g. Madsen [32] or Pawitan [33] for an introduction to maximum likelihood methods.

4.1. The maximum likelihood principle

Given the sequence of observations $\mathcal{Y}_N = \{\mathbf{Y}_i\}_{i=1}^N, \mathbf{Y}_k = \left[y_k^i, y_k^h, y_k^{\text{ret}}\right]^\intercal \in \mathbb{R}^{n_y}$, and set-points $\mathcal{U}_{N-1} = \{T_{\text{set},i}\}_{i=0}^{N-1}$, define the likelihood function as the product of the one-step ahead conditional densities:

$$\mathcal{L}(\boldsymbol{\theta}|\mathcal{Y}_N, \mathcal{U}_{N-1}) = p(\mathbf{X}_0)\prod_{k=1}^N p(\mathbf{Y}_k|\mathcal{Y}_{k-1}, \mathcal{U}_{k-1}, \boldsymbol{\theta}). \tag{19}$$

Here, p is the probability of observing $\mathbf{Y}_k$ given the previous observations, set-points, and parameters $\boldsymbol{\theta}$. $\mathbf{X}_0$ is the initial state of the system at time t_0. For linear stochastic differential equations, where the noise is state-independent and driven by Brownian motion, the conditional densities are also Gaussian. For non-linear systems though, this is not the case and the analytical density is in general hard (or impossible) to find. But when the time between observations are small, the Gaussian density approximates the analytical (unknown) density well. This motivates our choice of using the Gaussian density in the likelihood function. The Gaussian density is completely characterised by its conditional mean and variance; by introducing the one-step prediction error

$$\boldsymbol{\epsilon}_k = \mathbf{Y}_k - \hat{\mathbf{Y}}_{k|k-1}, \tag{20}$$

where $\hat{\mathbf{Y}}_{k|k-1} = \mathrm{E}[\mathbf{Y}_k|\mathcal{Y}_{k-1}, \mathcal{U}_{k-1}, \boldsymbol{\theta}]$, and the associated covariance $\mathbf{R}_{k|k-1} = \mathrm{Var}[\mathbf{Y}_k|\mathcal{Y}_{k-1}, \mathcal{U}_{k-1}, \boldsymbol{\theta}]$, we can write the likelihood function as

$$\mathcal{L}(\boldsymbol{\theta}|\mathcal{Y}_N, \mathcal{U}_{N-1}) = p(\mathbf{X}_0)\prod_{k=1}^N \frac{\exp\left(-\frac{1}{2}\boldsymbol{\epsilon}_k^\intercal \mathbf{R}_{k|k-1}^{-1}\boldsymbol{\epsilon}_k\right)}{\sqrt{\det(\mathbf{R}_{k|k-1})(2\pi)^{n_y}}}. \tag{21}$$

Taking the logarithm on both sides, we obtain the log-likelihood function

$$\ell(\boldsymbol{\theta}|\mathcal{Y}_N, \mathcal{U}_{N-1}) = \log\left(p(\mathbf{X}_0|\boldsymbol{\theta})\right) - \frac{1}{2}\sum_{k-1}^N \boldsymbol{\epsilon}_k^\intercal \mathbf{R}_{k|k-1}^{-1}\boldsymbol{\epsilon}_k + \log\left(\det(\mathbf{R}_{k|k-1})(2\pi)^{\frac{n_y}{2}}\right) \tag{22}$$

The log-likelihood has some attractive advantages over the ordinary likelihood when it comes to numerical properties, which is why it is often preferred. First, the sums are typically easier to deal with e.g. for differentiation and integration purposes. Second, the elimination of the exponential functions makes the optimisation The logari.thm is a monmore robustotonous transformation and thus does not change the point of the maximum. The parameter estimates $\hat{\boldsymbol{\theta}}$ is found by maximising the log-likelihood function

$$\hat{\boldsymbol{\theta}} = \arg\max_{\boldsymbol{\theta}} \ell(\boldsymbol{\theta}|\mathcal{Y}_N, \mathcal{U}_{N-1}) \tag{23}$$

To evaluate the log-likelihood function, we need to compute the one-step prediction errors, $\boldsymbol{\epsilon}_k$, and the associated covariance $\mathbf{R}_{k|k-1}$ (due to our assumption of Gaussian densities). The continuous-discrete extended Kalman filter supplies exactly these.

Table 2
The parameter estimates together with their statistical properties

Parameter	Estimate	95% confidence interval	Unit
T_{offset}	−0.101	[-0.081, −0.121]	[°C]
C_h	0.134	[0.128, 0.140]	[kJ/°C]
C_f	0.198	[0.194, 0.202]	
R_{fr}	2.030	[1.898, 2.162]	[°C h/ kJ]
C_i	9.57	[9.40, 9.742]	[kJ/°C]
C_w	45.36	[42.80, 47.92]	[kJ/°C]
R_{ih}	2.151	[2.121, 2.181]	[°C h/ kJ]
R_{iw}	0.199	[0.195, 0.203]	[°C h/ kJ]
R_{wa}	2.251	[1.775, 2.727]	[°C h/ kJ]
A_s	7.600	[-1.443, 16.64]	[m^2]
σ_1	8.6e-4	[9.7e-5, 0.008]	[°C]
σ_2	0.429	[0.419, 0.439]	[°C]
σ_3	111.6	[107.6, 118.0]	[kg/h]
σ_4	1.647	[1.144, 2.370]	[°C]
σ_5	6.469	[6.327, 6.612]	[°C]
R_1	9.6e-7	[1.1e-7, 8.5e-6]	[°C]
R_2	2.7e-4	[5.2e-6, 0.014]	[kW]
R_3	5.4e-3	[1.4e-3, 0.021]	[°C]
$\Phi_{\max}$	1145.3	[1133.5, 1157.1]	[kg/h]
α	1.592	[1.550, 1.634]	[1/°C]

4.2. The continuous-discrete extended Kalman filter

The continuous-discrete extended Kalman filter (CDEKF) is a variant of the celebrated Kalman filter [34]. It considers system models governed by continuous-time dynamics where the observer observers parts of the system at discrete times. In short, the CDEKF consists of a *prediction* step and an *update* step. The extended Kalman filter relies on a linearisation of the non-linear system (1), which causes troubles if g is state-dependent. In such cases, the Lamperti-transformation is an important tool to transform (1) into a state-independent SDE [35,36]. The literature contains many introductions and applications to Kalman filtering and the CDEKF, see e.g. [37,19].

4.2.1. The prediction scheme

In this step, the CDEKF predicts the state of the building $\widehat{bfX}_{k|k-1} = \mathrm{E}\left[\mathbf{X}_k|\mathcal{Y}_{k-1}, \mathcal{U}_{k-1}, \hat{\boldsymbol{\theta}}\right], \mathbf{X}_k = \left[T^i_{t_k}, T^w_{t_k}, \Phi_{t_k}, T^h_{t_k}, T^{\text{ret}}_{t_k}\right]^\intercal$, together with the state covariance $\widehat{P}_{k|k-1} = \mathrm{Var}\left[\mathbf{X}_k|\mathcal{Y}_{k-1}, \mathcal{U}_{k-1}, \hat{\boldsymbol{\theta}}\right]$ at the next time step t_k given the estimated state at time t_{k-1}, $\widehat{bfX}_{k|k-1}$. This involves solving a set of coupled ordinary differential equations (ODEs). Any ODE-solver is sufficient for this task.

4.2.2. The update scheme

The updating scheme is about estimating the underlying state and its covariance, denoted $\widehat{bfX}_{k|k}$ and $\widehat{P}_{k|k}$, at the next time instance t_k, given our predictions, $\widehat{bfX}_{k|k-1}$ and $\widehat{P}_{k|k-1}$, and an observation $\mathbf{Y}_k$. Informally speaking, the updating scheme finds a weight K, typically called the *Kalman gain*, which "measures" how much weight the observation should have on the estimate $\widehat{bfX}_{k|k}$. Consider the update equations for the state estimate

$$\widehat{bfX}_{k|k} = \widehat{bfX}_{k|k-1} + K\boldsymbol{\epsilon}_k. \tag{24}$$

If K is small, the prediction weights more compared to the observation in the estimate of the state. The covariance of the one-step prediction error, $\mathbf{R}_{k|k-1}$, is usually calculated in the updating scheme as well. With $\boldsymbol{\epsilon}_k$ and $\mathbf{R}_{k|k-1}$ at hand, we can evaluate the conditional density associated with the k'th observation. This recursion is applied to all observations in $\mathcal{Y}_N$, and with a given initial condition $\mathbf{X}_0$, the log-likelihood in (22) can be computed.

4.3. Details in the parameter estimation

As previously described, the return temperature exhibits inconsistent behaviour when the heat load is zero. Also, at these times, the return temperature is not of interest for control purposes. For these reasons, we choose to disregard the return temperature in the parameter estimation at times where the heat load is zero. That is, we need to ensure that the return temperature for these times does not affect the likelihood function. We thus add a very large constant (say 10^{20}) to the observation variance in the Kalman filter when the heat load is close to zero (say < 0.01 [kW]). As a result, the *observed* return temperature has negligible effect on the likelihood estimates during these times. Such actions are crucial to implement for applications in general, e.g. MPC, where indescrib-

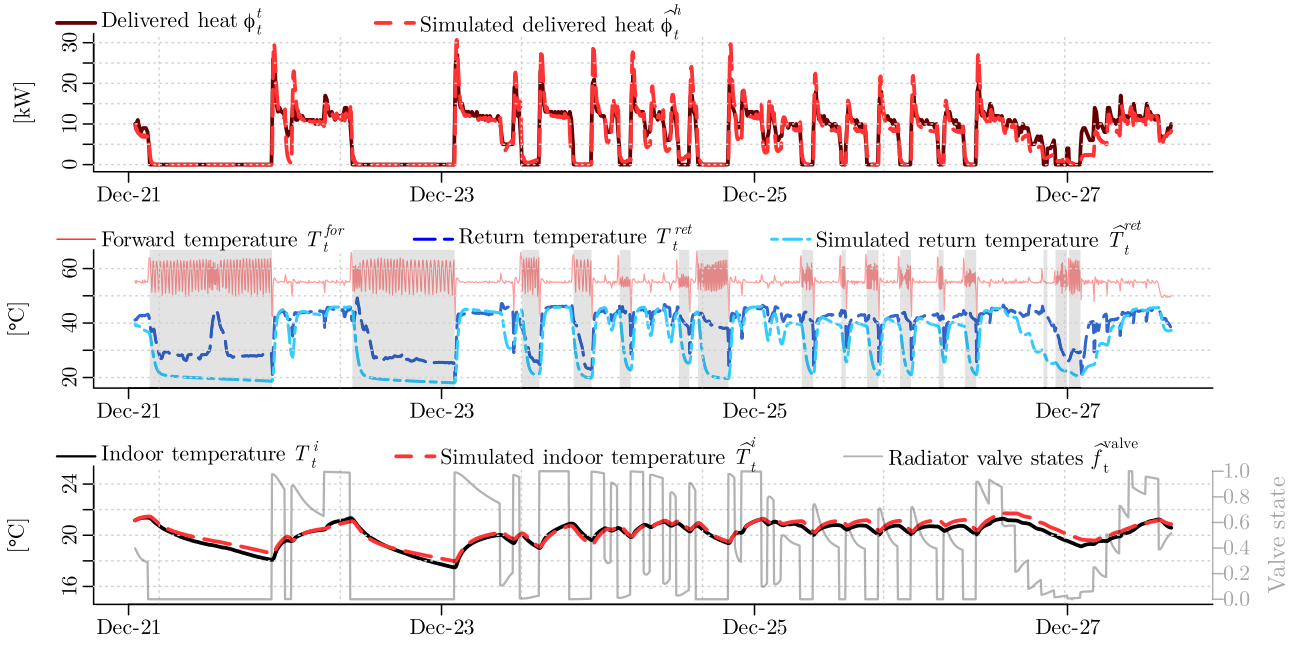

Fig. 5. A simulation of the resulting model: given initial conditions, the model predicts the entire week. The model performs well given the long prediction horizon. The grey periods in the second plot depicts the periods where the observation variance on the return temperature is large.

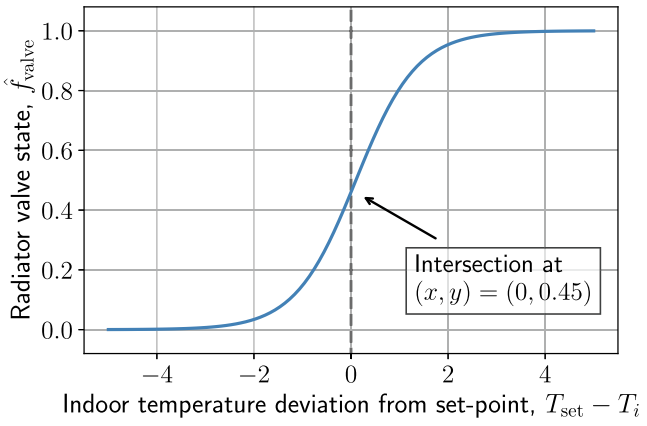

Fig. 6. The estimated valve function.

able dynamics occur or observations are not of interest and a Kalman filter is applied for state estimation. The larger variance on the observed return temperature ensures that it contributes very little to the state estimate at that point in time.

To evaluate the log-likelihood in Eq. (22), this paper uses the software CTSM-R [38]. To maximise Eq. (23), we use Nelder-Mead routine in the `NLopt` optimisation library in `R` [39]. On average, the estimation took between 3 and 8 min until convergence (to a minimum) using a computer with an Intel Core i7-8665U processor with 8 cores clocked at 1.90 GHz. In total, we estimated 20 parameters.

5. Results and discussion

This section presents the results in terms of parameter estimates, simulation of the model, and residual analysis. We compare a simulation of the model with the experiment data to see the model's performance over the entire data set given only the initial conditions. For the simulations, we use the same weather observations and set-points as inputs. Finally, we discuss the capabilities and strengths/weaknesses of the model.

5.1. Simulation results

Table 2 displays the parameter estimates for the model presented in Section 3. All parameters are strongly significant, except the solar radiation gain A_s. The explanation is likely that the data contains no significant solar radiation. The parameter thus becomes hard to determine without large uncertainty. But the solar radiation gain is an important disturbing factor for building climate control [40]. We thus intend to describe the solar radiation gain better in the future, when more experiments/data are available. The literature contains interesting approaches to model this, such as using B-splines to describe the varying solar gain during the day [41].

Fig. 5 shows a simulation of the experiment given only the initial states. The model does a good job for all three variables. It predicts long into the future and still shows good accuracy without large drifts. That is, the model performs very well on long prediction horizons. This is crucial for the performance of MPC. This simulation, however, uses the same weather disturbances as the data. For practical purposes, weather forecasts are not perfect, which affects the prediction performance [42,43].

The predicted heat was a challenge to model, but the simulation suggests that the model captures the most crucial dynamics. However, the simulation also indicates that the model is not able to "turn off" the delivered heat fast enough compared to data, as it seems to go slower to zero. This flaw comes from the fact that we model the flow as an SDE itself, Φ_t. Thus, the flow goes expo-

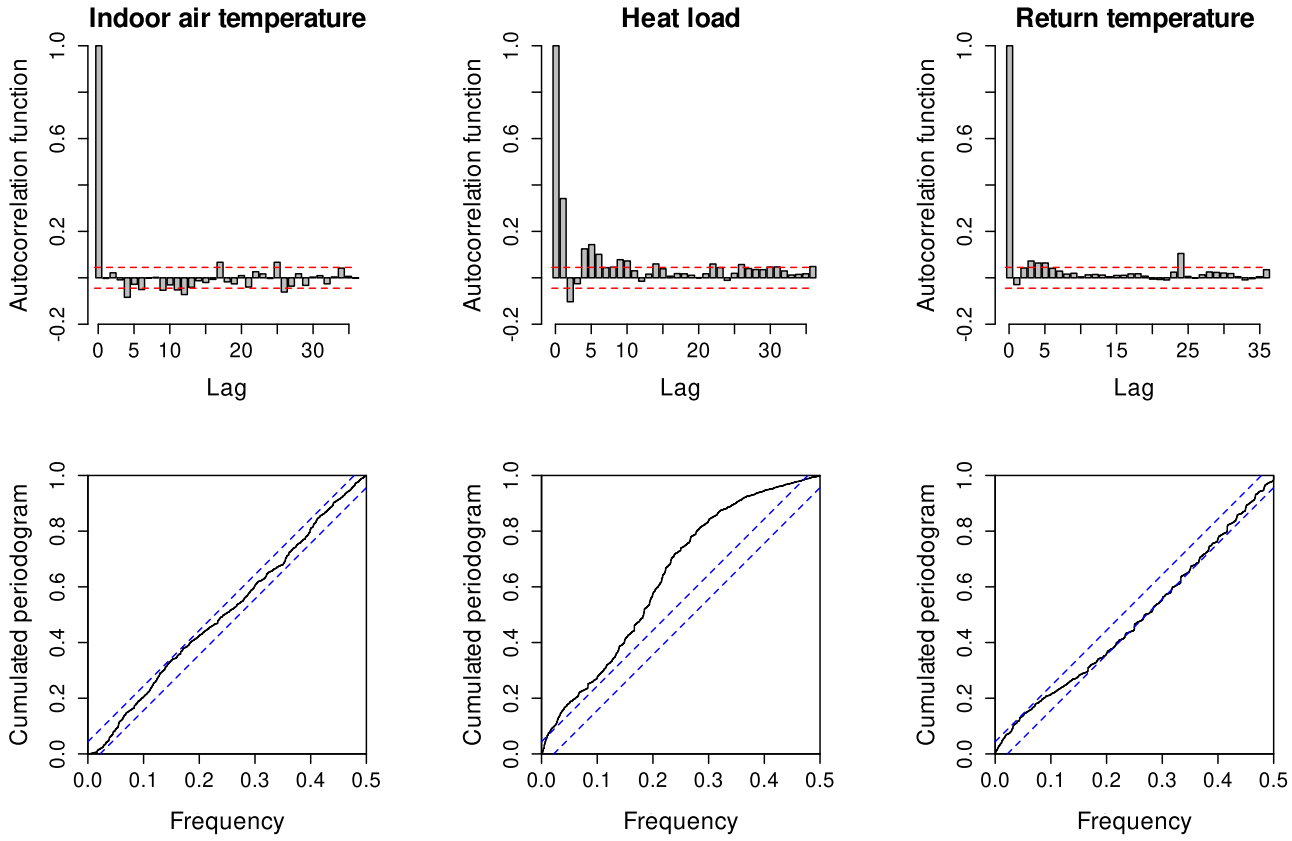

Fig. 7. The estimated autocorrelation function and the cumulated periodogram of the 1-step prediction errors. Each column corresponds to a variable.

nentially towards the term $\Phi_{max} f_t^{valve}$ (which in theory never equals zero due to the sigmoid curve). Fig. 6 shows the estimated valve state as a function of the deviation of the set point. The trancient state from closed to open is approximately 5 °C and at equilibrium the valve state is below 0.5, which are both expected for a typical thermostat [25].

We found that the dynamics of the return temperature were hard to mimic and capture, especially when the heat is turned off. Fig. 5 confirms that we are somewhat capable of predicting the return temperature whenever the heating system is turned on. The indoor air temperature in Fig. 5 seems to catch the overall dynamics of the data. The building model, however, does seem to be a bit too well insulated by the looks of the long periods where no heat is delivered. The simulated temperature decreases slower compared to data. Also, from around December 25th and onwards, the simulated indoor air temperature seems to drift a bit upwards compared to data. In this period, the estimated valve states are never fully opened, indicating that the set-point and observed temperatures are very close. Thus, the upwards drift of the simulation could come from the sigmoid curve of the valve function, since it never fully closes and is still open even when the observed temperature is above the set-point.

5.2. Residual analysis

Fig. 7 shows the estimated autocorrelation function and the cumulated periodogram of the 1-step prediction errors for each of the variables. Both the autocorrelation function and the cumulated periodogram indicate that the residuals of the indoor air temperature and the return temperature can be classified as white noise. However, the heat load residuals are governed by some minor autocorrelation in the first few lags. Inspection of the spectral density and the residual plots confirms that non-uniformity of the spectrum primarily comes from the heater state's exponential decay towards zero when the heat is turned off. However, this is a minor autocorrelation that is not going to impact MPC performance significantly.

5.3. Future work

Since the experiment took place during the Christmas holiday, the building was not occupied at any time. However, human occupancy/behaviour is important to model and include in MPC [44]. Also, due to the lag of occupancy, we do not know how open windows affect the indoor air temperature. These are important topics to investigate further to accurately model the thermal dynamics of the building [45].

6. Conclusion

This paper introduced a physically inspired SDE-based nonlinear model to describe the complex heat dynamics of a school building with water-based heating. The purpose of the model is to predict the indoor air temperature, the heat load, and the return temperature of the water in the space heating (SH) system. We model the thermostats in the radiators using a Sigmoid function to describe the level of water flow through the radiators. We fitted the parameters in the model from time-series data using maximum likelihood estimation. To validate the estimated model, we compared a simulation of the model, only given the initial conditions and disturbances, to data. This showed great accuracy over an entire week. The residual analysis indicated that the model lacks some dynamical descriptions of the heat load. We believe the reason might be that the model does not shut down the heat load fast enough. Beside this, the model looks promising for enabling MPC and e.g. embedded forecasts.

Declaration of Competing Interest

The authors declare that they have no known competing financial interests or personal relationships that could have appeared to influence the work reported in this paper.

Acknowledgement

The authors received funding from the following projects; *Sustainable plus energy neighbourhoods (syn.ikia)* (H2020 No. 869918), *Centre for IT-Intelligent Energy Systems (CITIES)* (DSF 1305-00027B), Top-Up (Innovation Fund Denmark 9045-00017B), SCA+ (Interreg Öresund-Kattegat-Skagerrak), *Research Centre on Zero Emission Neighbourhoods in Smart Cities (FME-ZEN)* (Research Council of Norway, No. 257660), and *Flexibile Energy Denmark (FED)* (IFD 8090-00069B).

References

[1] M.Z. Hauschild, S. Kara, I. Røpke, Absolute sustainability: Challenges to life cycle engineering, CIRP Ann. 69 (2) (2020) 533–553, https://doi.org/10.1016/j.cirp.2020.05.004.
[2] D.W. O'Neill, A.L. Fanning, W.F. Lamb, J.K. Steinberger, A good life for all within planetary boundaries, Nat. Sustain. 1 (2) (2018) 88–95, https://doi.org/10.1038/s41893-018-0021-4.
[3] N. O'Connell, P. Pinson, H. Madsen, M. O'Malley, Benefits and challenges of electrical demand response: a critical review. Renew. Sustain Energy Rev. 2014;39:686–699, ISSN 18790690, 13640321. doi:10.1016/j.rser.2014.07.098..
[4] Østergaard Jensen S, Parker J, Engelmann P, Joanna A. Examples of energy flexibility in buildings [Tech. Rep.]; 2019..
[5] G. Serale, M. Fiorentini, A. Capozzoli, D. Bernardini, A. Bemporad, Model Predictive Control (MPC) for Enhancing Building and HVAC System Energy Efficiency: Problem Formulation, Applications and Opportunities, Energies 11 (3) (2018) 631, ISSN 1996–1073, doi:10.3390/en11030631..
[6] J. Drgoňa, J. Arroyo, I. Cupeiro Figueroa, D. Blum, K. Arendt, D. Kim, E.P. Ollé, J. Oravec, M. Wetter, D.L. Vrabie, L. Helsen, All you need to know about model predictive control for buildings, Annual Reviews in Control..
[7] D. Cali, D. Müller, H. Madsen, Benefits of the Inclusion of Occupant Behaviour Profiles in the Simulation of the Energy Performance of Buildings, in: Proceedings of 16th IBPSA International Conference & Exhibition Building Simulation 2019, url:http://buildingsimulation2019.org, building Simulation 2019, BS 2019; Conference date: 02-09-2019 Through 04-09-2019, 2019..
[8] S. Wolf, D. Cali, M. Alonso, R. Li, R. Andersen, J. Krogstie, H. Madsen, Room-level Occupancy Simulation Model for Private Households, vol. 1343, IOP Publishing, ISSN 1742–6596, url:https://cisbat.epfl.ch/, cISBAT 2019: Climate Resilient Cities - Energy Efficiency & Renewables in the Digital Era, CISBAT 2019; Conference date: 04-09-2019 Through 06-09-2019, 2019..
[9] A. Duun-Henriksen, S. Schmidt, R. Røge, J. Møller, K. Nørgaard, J. Jørgensen, H. Madsen, Model Identification Using Stochastic Differential Equation Grey-Box Models in Diabetes, J. Diabetes Sci. Technol. 7 (2013) 431–440, https://doi.org/10.1177/193229681300700220.
[10] A. Afram, F. Janabi-Sharifi, Gray-box modeling and validation of residential HVAC system for control system design, Appl. Energy 137 (2015) 134–150, https://doi.org/10.1016/j.apenergy.2014.10.026.
[11] S. Wang, X. Xu, Simplified building model for transient thermal performance estimation using GA-based parameter identification, Int. J. Thermal Sci. 45 (4) (2006) 419–432, https://doi.org/10.1016/j.ijthermalsci.2005.06.009.
[12] M. Massano, E. Macii, E. Patti, A. Acquaviva, L. Bottaccioli, A Grey-box Model Based on Unscented Kalman Filter to Estimate Thermal Dynamics in Buildings, in: 2019 IEEE International Conference on Environment and Electrical Engineering and 2019 IEEE Industrial and Commercial Power Systems Europe (EEEIC/ I CPS Europe), 1–6, 2019..
[13] P. Bacher, H. Madsen, Identifying suitable models for the heat dynamics of buildings, Energy and Buildings 43 (7) (2011) 1511–1522, ISSN 0378–7788, doi:10.1016/j.enbuild.2011.02.005..
[14] A. Scott, The Nonlinear Universe, Springer, Berlin, Heidelberg, 2007.
[15] M. Jiménez, H. Madsen, J. Bloem, B. Dammann, Estimation of non-linear continuous time models for the heat exchange dynamics of building integrated photovoltaic modules, Energy Buildings 40 (2) (2008) 157–167, https://doi.org/10.1016/j.enbuild.2007.02.026.
[16] C. Lodi, P. Bacher, J. Cipriano, H. Madsen, Modelling the heat dynamics of a monitored Test Reference Environment for Building Integrated Photovoltaic systems using stochastic differential equations, Energy and Buildings 50 (2012) 273 – 281, ISSN 0378-7788, doi:10.1016/j.enbuild.2012.03.046..
[17] E. Wernholt, S. Gunnarsson, NONLINEAR GREY-BOX IDENTIFICATION OF INDUSTRIAL ROBOTS CONTAINING FLEXIBILITIES, IFAC Proceedings Volumes

38 (1) (2005) 356–361, ISSN 1474–6670, doi:10.3182/20050703-6-CZ-1902.00060, 16th IFAC World Congress..
[18] J.K. Møller, H. Madsen, J. Carstensen, Parameter estimation in a simple stochastic differential equation for phytoplankton modelling, Ecological Modelling 222 (11) (2011) 1793–1799, ISSN 0304–3800, doi:10.1016/j.ecolmodel.2011.03.025..
[19] B. Øksendal, Stochastic Differential Eqs, 3rd Ed., An Introduction with Applications, Springer-Verlag, Berlin, Heidelberg, 1992.
[20] D. Boiroux, J.B. Jørgensen, A Nonlinear Model Predictive Control Strategy for Glucose Control in People with Type 1 Diabetes, IFAC-PapersOnLine 51 (27) (2018) 192–197.
[21] C.A. Thilker, R.G. Junker, P. Bacher, J.B. Jørgensen, H. Madsen, Model predictive control based on stochastic differential equations, in: C. Ghiaus, M. Amayri, S. Ploix (Eds.), Towards Energy Smart Homes: Algorithms, technologies, and applications, Springer, publication expected in 2021, 2021..
[22] P.A. Stentoft, T. Munk-Nielsen, L. Vezzaro, H. Madsen, P.S. Mikkelsen, J.K. Møller, Towards model predictive control: online predictions of ammonium and nitrate removal by using a stochastic ASM, Water Sci. Technol. 79 (1) (2018) 51–62.
[23] B. Xu, L. Fu, H. Di, Dynamic simulation of space heating systems with radiators controlled by TRVs in buildings, Energy and Buildings 40 (9) (2008) 1755–1764, ISSN 0378–7788, doi:10.1016/j.enbuild.2008.03.004..
[24] M.S. Mohseni, D. Gotthardsson, R. Høallbus, H. Vallmark, Analysis of the Thermal Performance of Hydronic Radiators and Building Envelop: Developing Experimental (Step Response) and Theoretical Models and Using Simulink to Investigate Different Control Strategies, Civil Engineering Research Journal 2 (4), doi:10.19080/CERJ.2017.02.555595..
[25] L.H. Hansen, Stochastic modelling of central heating systems, Ph.D. thesis, Technical University of Denmark, url:http://www2.imm.dtu.dk/pubdb/pubs/2460-full.html, 1997..
[26] C.G. Bruun, Optimization of Building Operation Using High-resolution Sensor Data, Master's thesis, Technical University of Denmark, Department of Civil Engineering, can be found at https://www.findit.dtu.dk, 2019..
[27] H. Madsen, J. Holst, Estimation of continuous-time models for the heat dynamics of a building, Energy Building 22 (1995) 67–79.
[28] K.K. Andersen, H. Madsen, L.H. Hansen, Modelling the heat dynamics of a building using stochastic differential equations, Energy Buildings 31 (1) (2000) 13–24.
[29] B. Nielsen, H. Madsen, Identification of a Linear Continuous Time Stochastic Model of the Heat Dynamics of a Greenhouse, Journal of Agricultural Engineering Research 71 (3) (1998) 249–256, ISSN 0021–8634, doi:10.1006/jaer.1998.0322..
[30] O. Brastein, D. Perera, C. Pfeifer, N.-O. Skeie, Parameter estimation for grey-box models of building thermal behaviour, Energy and Buildings 169 (2018) 58 – 68, ISSN 0378-7788, doi:10.1016/j.enbuild.2018.03.057..
[31] H. Harb, N. Boyanov, L. Hernandez, R. Streblow, D. Møller, Development and validation of grey-box models for forecasting the thermal response of occupied buildings, Energy Buildings 117 (2016) 199–207, https://doi.org/10.1016/j.enbuild.2016.02.021.
[32] H. Madsen, Time series analysis, Chapman & Hall, 2007.
[33] Y. Pawitan, In All Likelihood: Statistical Modelling and Inference Using Likelihood, Clarendon Press, Oxford, 2006.
[34] R.E. Kalman, A New Approach to Linear Filtering and Prediction Problems, J. Basic Eng. 82 (1) (1960) 35–45.
[35] J.K. Møller, H. Madsen, From State Dependent Diffusion to Constant Diffusion in Stochastic Differential Equations by the Lamperti Transform, IMM-Technical Report-2010-16, Technical University of Denmark, DTU Informatics, Building 321, 2010..
[36] C.A. Thilker, Optimization for Smart Energy Systems, Master's thesis, Technical University of Denmark, Department of Applied Mathematics and Computer Science, 2020..
[37] P. Frogerais, J.-J. Bellanger, L. Senhadji, Various Ways to Compute the Continuous-Discrete Extended Kalman Filter, IEEE Trans. Automatic Control - IEEE TRANS AUTOMAT CONTR 57 (2012) 1000–1004, https://doi.org/10.1109/TAC.2011.2168129.
[38] R. Juhl, N.R. Kristensen, P. Bacher, J. Kloppenborg, H. Madsen, CTSM-R User Guide, technical University of Denmark, 2013..
[39] S.G. Johnson, The NLopt nonlinear-optimization package, url:http://github.com/stevengj/nlopt, 2020..
[40] T. Mingfang, Solar control for buildings, Building Environ. 37 (7) (2002) 659–664, https://doi.org/10.1016/S0360-1323(01)00063-4.
[41] C. Rasmussen, L. Frölke, P. Bacher, H. Madsen, C. Rode, Semi-parametric modelling of sun position dependent solar gain using B-splines in grey-box models, Solar Energy 195 (2020) 249–258.
[42] C. Thilker, H. Madsen, J. Jørgensen, Advanced forecasting and disturbance modelling for model predictive control of smart energy systems, Applied Energy 292, ISSN 0306–2619, doi:10.1016/j.apenergy.2021.116889..
[43] F. Oldewurtel, A. Parisio, C.N. Jones, D. Gyalistras, M. Gwerder, V. Stauch, B. Lehmann, M. Morari, Use of model predictive control and weather forecasts for energy efficient building climate control, Energy Buildings 45 (2012) 15–27, https://doi.org/10.1016/j.enbuild.2011.09.022.
[44] F. Oldewurtel, D. Sturzenegger, M. Morari, Importance of occupancy information for building climate control, Applied Energy 101 (2013) 521–532, doi:10.1016/j.apenergy.2012.06.014, sustainable Development of Energy, Water and Environment Systems..
[45] H.B. Rijal, P. Tuohy, F. Nicol, M.A. Humphreys, A. Samuel, J. Clarke, Development of an adaptive window-opening algorithm to predict the thermal comfort, energy use and overheating in buildings, J. Building Performance Simul. 1 (1) (2008) 17–30, https://doi.org/10.1080/19401490701868448.